Electronic Supplementary Material (ESI) for Journal of Materials Chemistry C.

Supporting Information

Improving the Efficiency and Stability of Inorganic Red Perovskite Light Emitting Diodes by Traces of Zinc Ions

Xiao-Yi Cai,[†1] Yi Yu,[†2] Yong-Chun Ye,[1] Yang Shen,[1] Ming-Lei Guo,[1] Jing-Kun Wang,[1] Kong-Chao Shen,[1] Yan-Qing Li,[2,*] Jian-Xin Tang[1,3*]

[1] *Institute of Functional Nano & Soft Materials (FUNSOM), Jiangsu Key Laboratory for Carbon-Based Functional Materials & Devices, Soochow University, Suzhou 215123, China, E-mail: jxtang@suda.edu.cn (J.X. Tang)*

[2] *School of Physics and Electronic Science, Ministry of Education Nanophotonics and Advanced Instrument Engineering Research Center, East China Normal University, Shanghai 200062, China, E-mail: yqli@phy.ecnu.edu.cn (Y.Q. Li)*

[3] *Macao Institute of Materials Science and Engineering, Macau University of Science and Technology, Taipa 999078, Macau SAR, China*

[†] These authors contributed equally to this work.

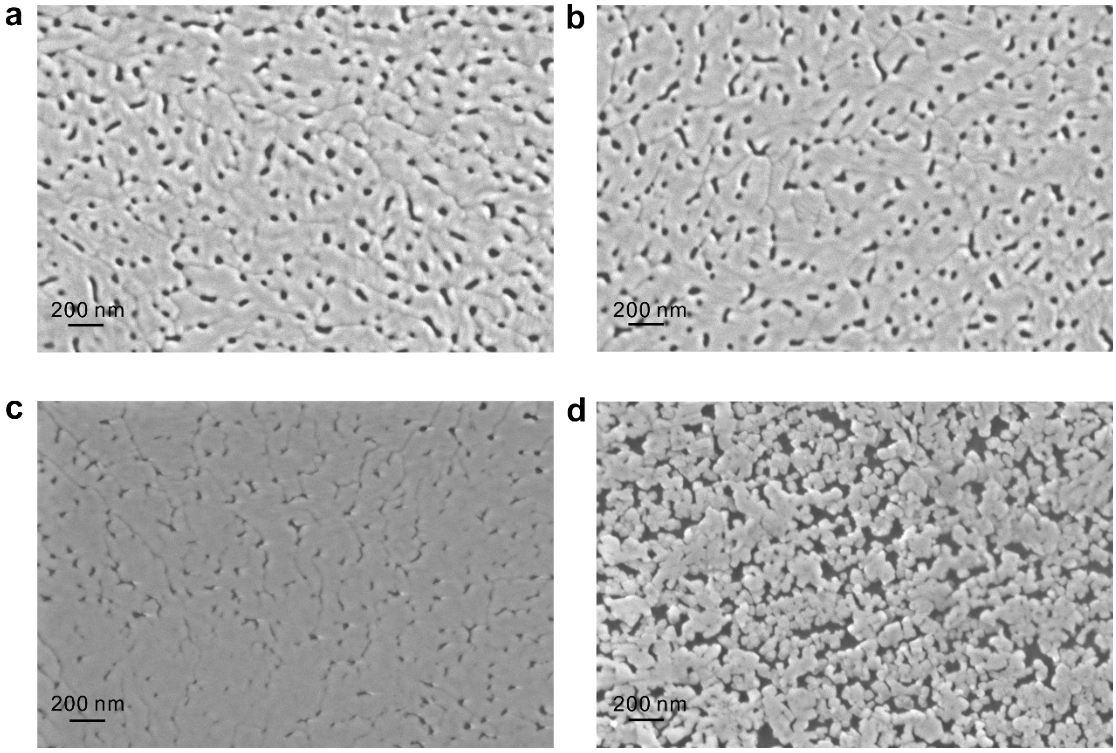

Figure S1. SEM images of the prepared $CsPbI_{3-x}Br_x$ films by adding different amounts of ZnI_2 into the precursor solution. (a) 0.0%, (b) 0.5%, (c) 1.0%, and (d) 1.5% molar ratio of Zn/Pb.

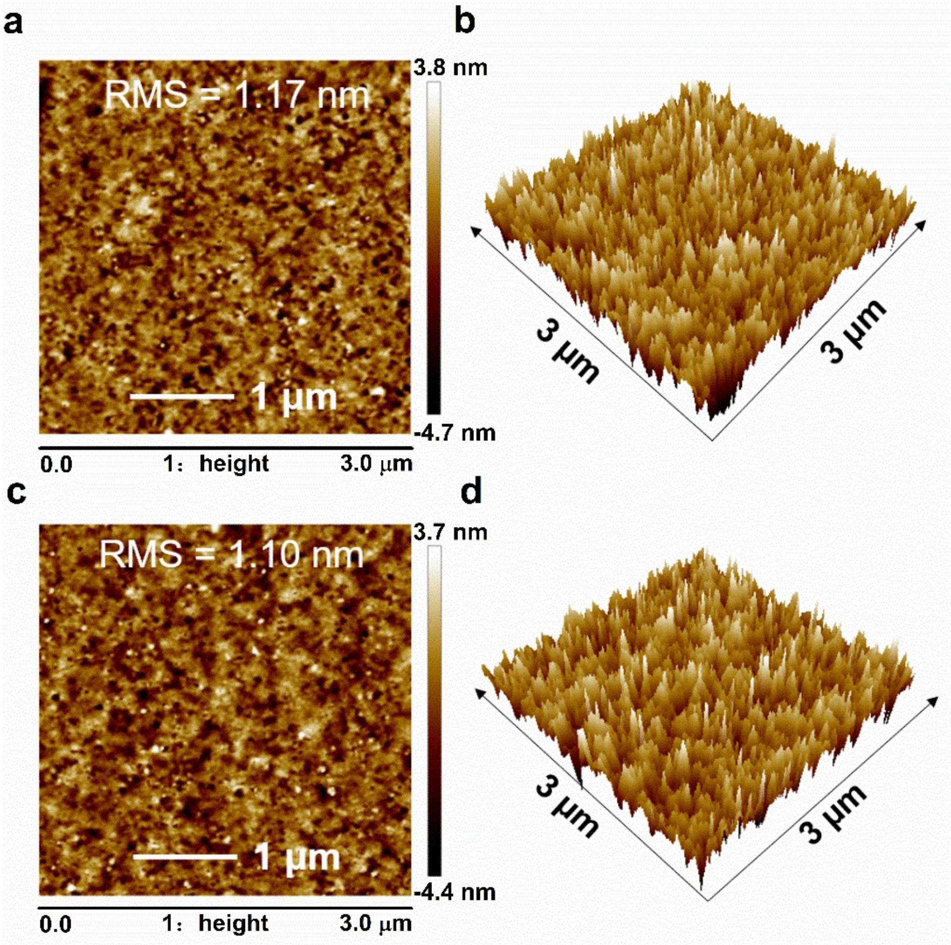

Figure S2. AFM images of the prepared perovskite films. Tapping-mode AFM images of the pristine $CsPbI_{3-x}Br_x$ film (a)(b). The film RMS roughness is about 1.17 nm, the scan area is 3 μm × 3 μm. Tapping-mode AFM images of the $CsPbI_{3-x}Br_x$ thin film incorporating with ZnI_2 (c)(d). The film RMS roughness is about 1.10 nm, the scan area is 3 μm × 3 μm.

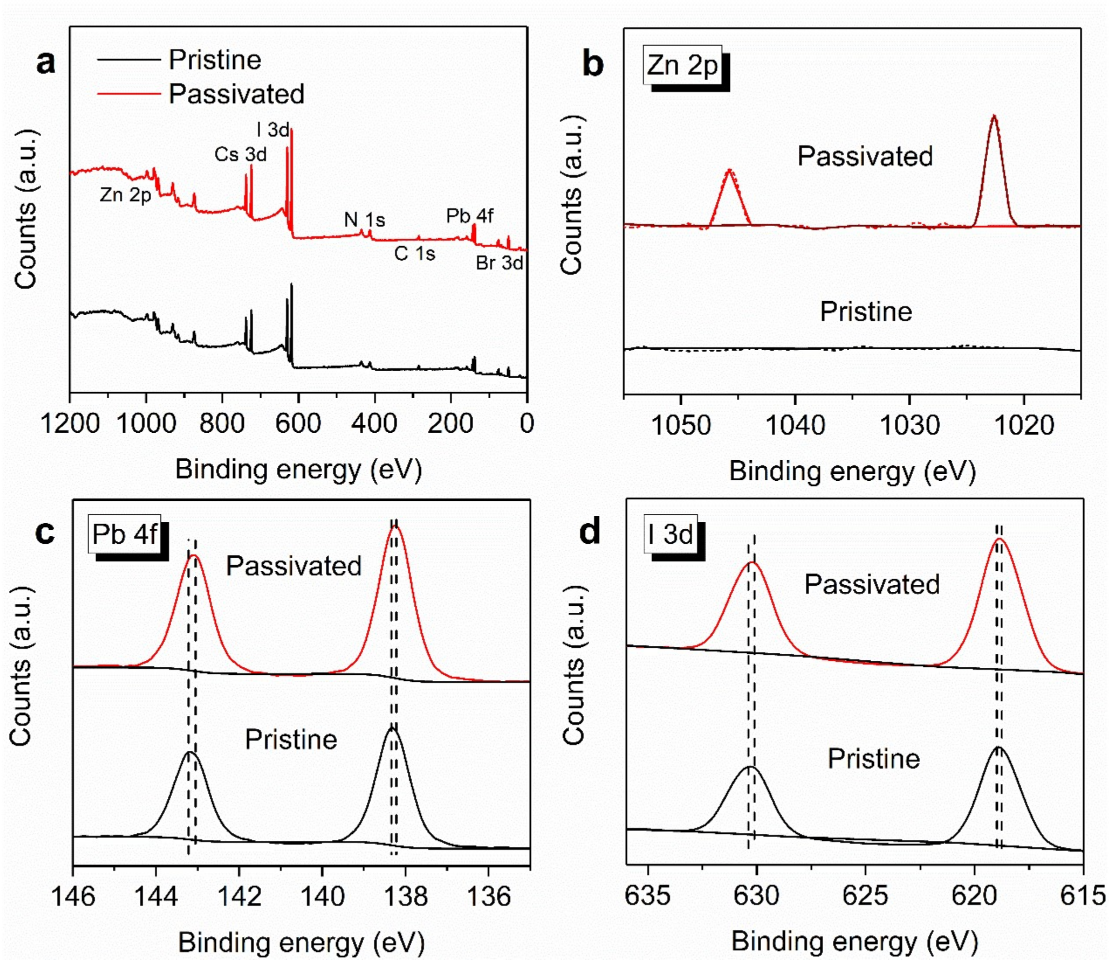

Figure S3. (a) XPS spectra of pristine and ZnI_2-passivated $CsPbI_{3-x}Br_x$ films. XPS analysis of pristine and ZnI_2-passivated films for (b) Zn 2p, (c) Pb 4f and (d) I 3d.

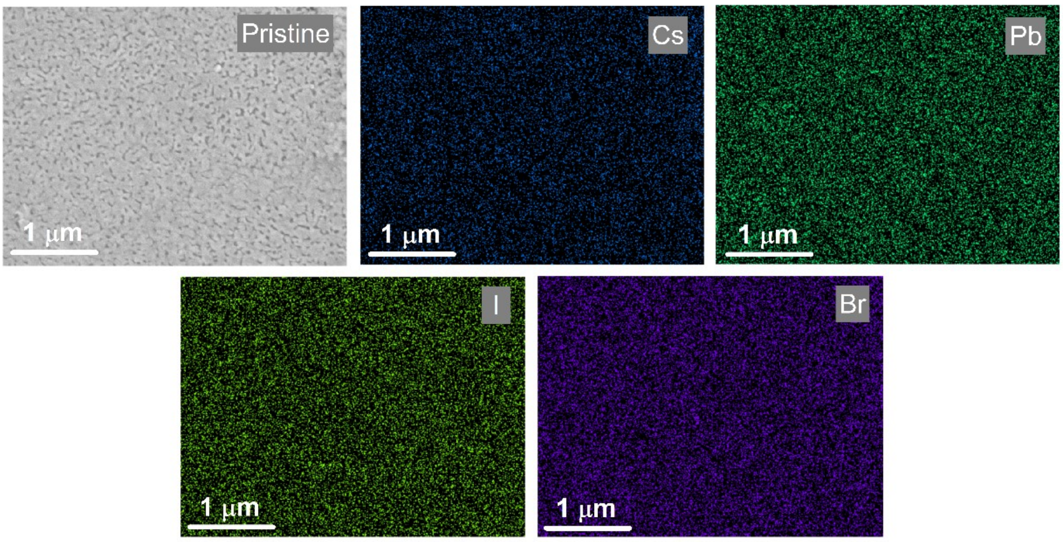

Figure S4. SEM image and corresponding elemental mapping images of pristine $CsPbI_{3-x}Br_x$ perovskite thin film. Scale bar: 1 μm.

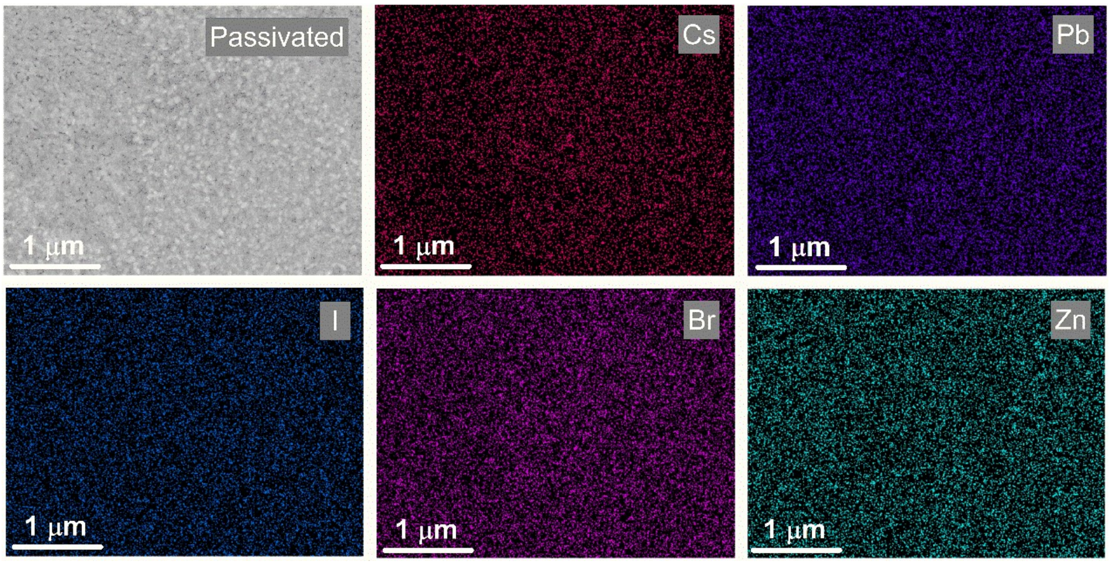

Figure S5. SEM image and corresponding elemental mapping images of passivated $CsPbI_{3-x}Br_x$ perovskite thin film. Scale bar: 1 μm.

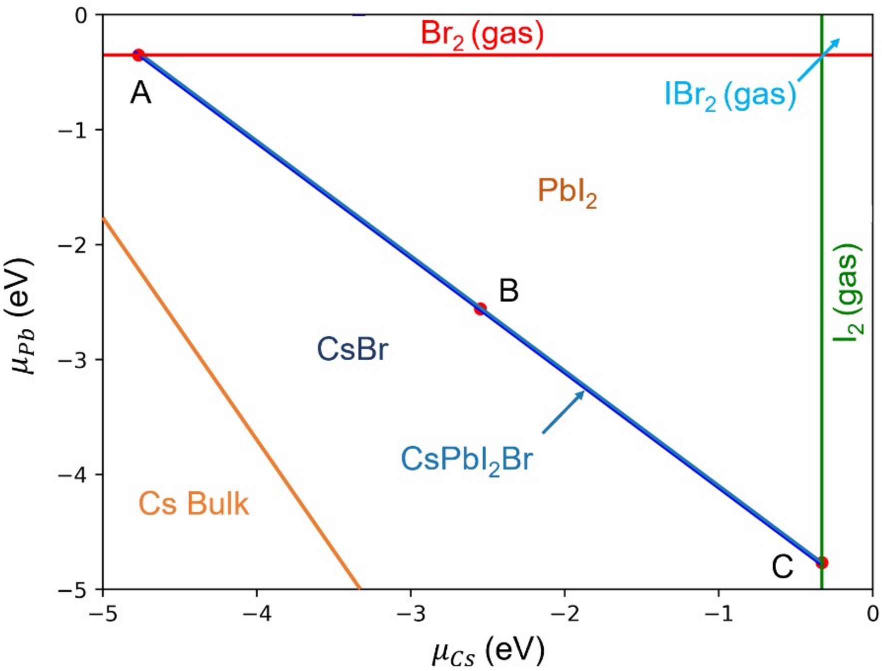

Figure S6. Stability regions of various compounds against Cs and Pb chemical potentials in $CsPbI_2Br$. The region indicates the available equilibrium chemical potential region for $CsPbI_2Br$. Three representative points (A: Br-rich/I-poor, B: moderate, C: I-rich/Br-poor conditions) are selected for the formation energy calculations.

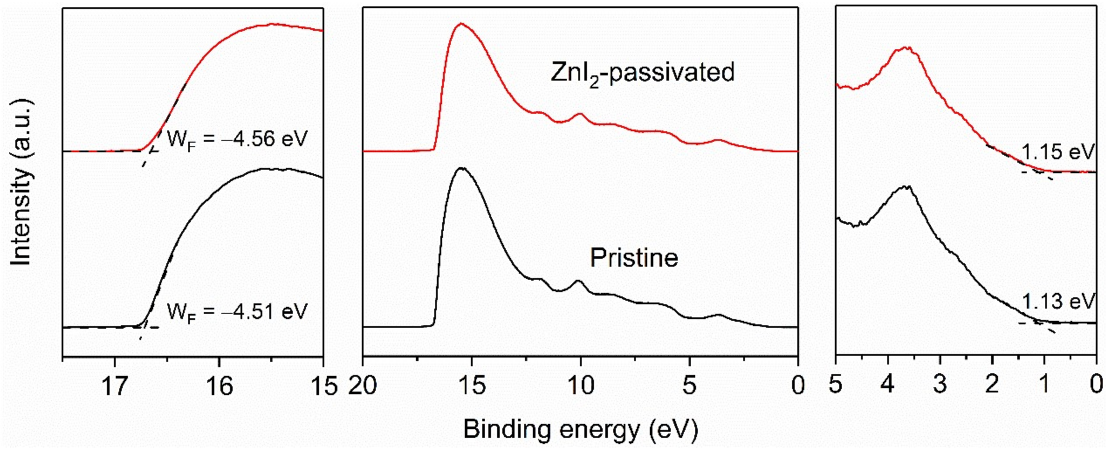

Figure S7. UPS spectra of the pristine $CsPbI_{3-x}Br_x$ and ZnI_2-passivated $CsPbI_{3-x}Br_x$ films. Their W_Fs are −4.51 eV and −4.56 eV, respectively. Their HOMOs are −5.71 eV and −5.64 eV, respectively.

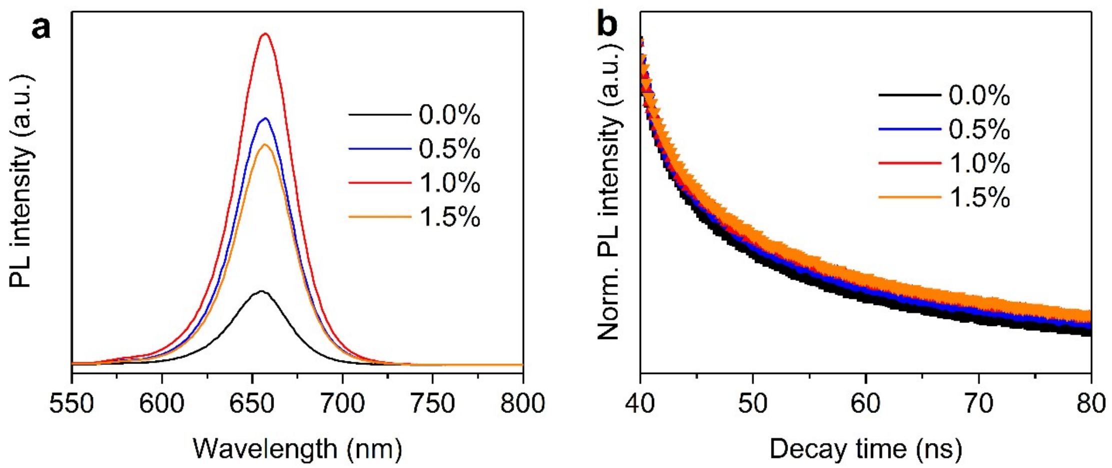

Figure S8. PL spectra (a) and TRPL spectra (b) of pristine and ZnI_2-passivated $CsPbI_{3-x}Br$ films with different molar ratio of Zn/Pb on PEDOT:PSS films.

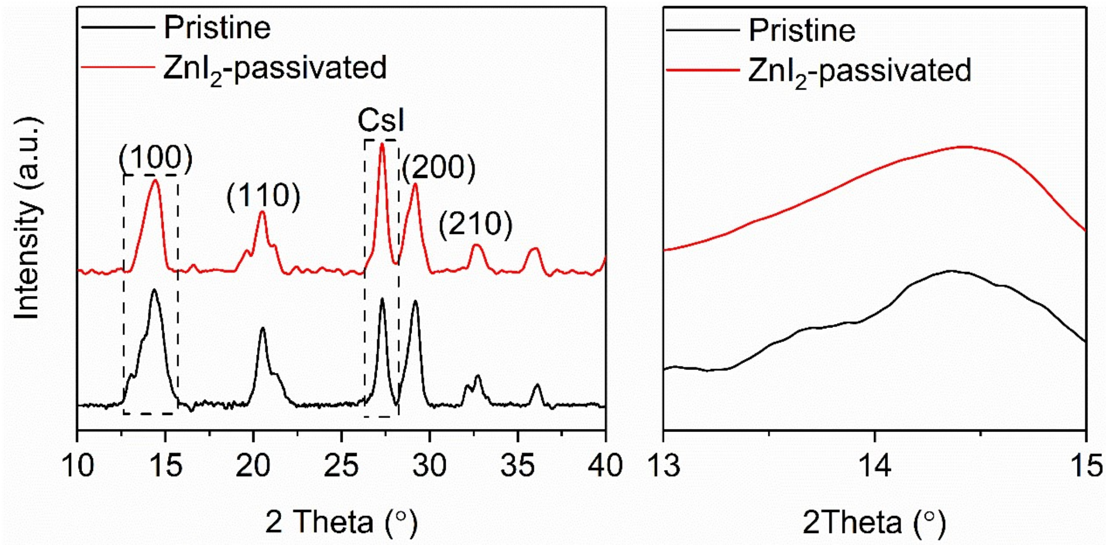

Figure S9. Comparison of the perovskite crystallinity. XRD patterns of the $CsPbI_{3-x}Br_x$ films with and without ZnI_2 passivation.

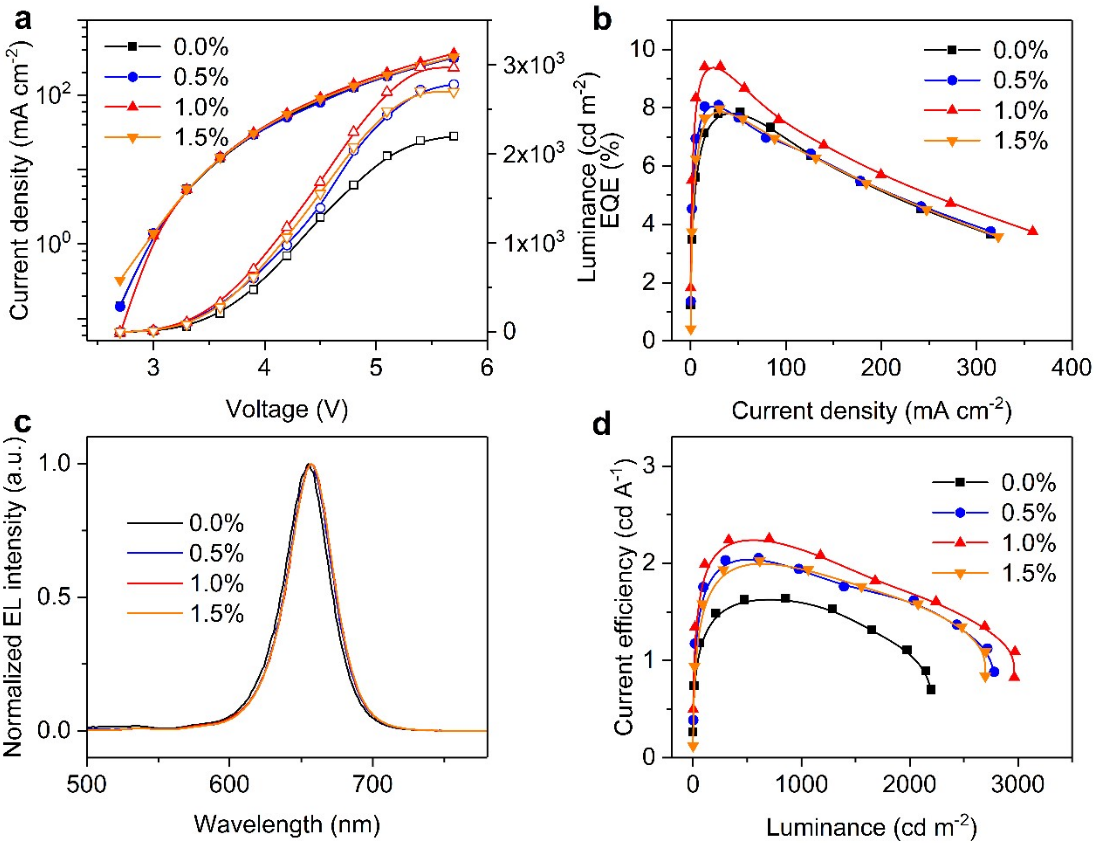

Figure S10. (a) J-V-L curves, (b) EQE versus current density curves, (c) EL spectra and (d) CE versus luminance of $CsPbI_{3-x}Br_x$ PeLEDs with different molar ratio of Zn/Pb.

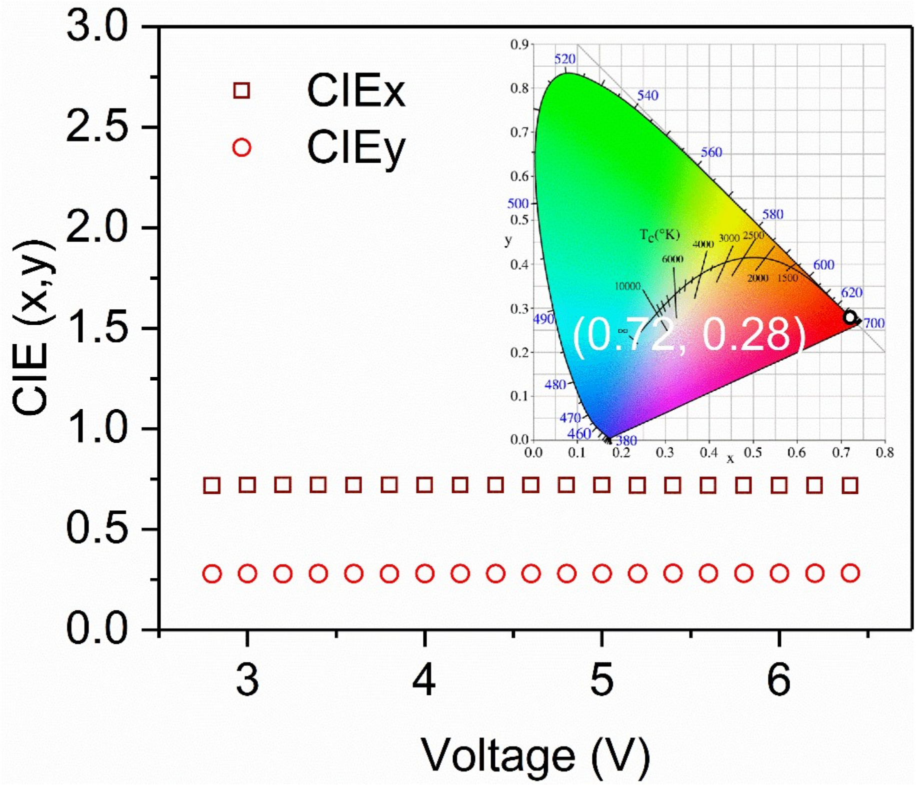

Figure S11. CIE coordinates of the ZnI_2-passivated $CsPbI_{3-x}Br_x$ PeLEDs under different bias voltages. Inset is CIE color coordinates under an applied voltage of 3.6 V.

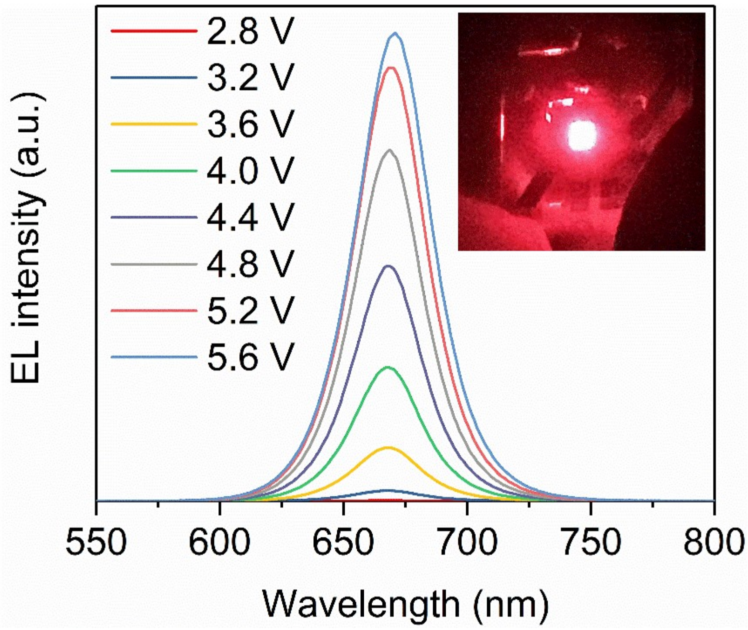

Figure S12. EL spectra of the ZnI_2-passivated $CsPbI_{3-x}Br_x$ based PeLEDs at the bias voltages from 2.8 V to 5.6 V. Inset is a photograph of red emission PeLED operating under 5.4 V forward bias.

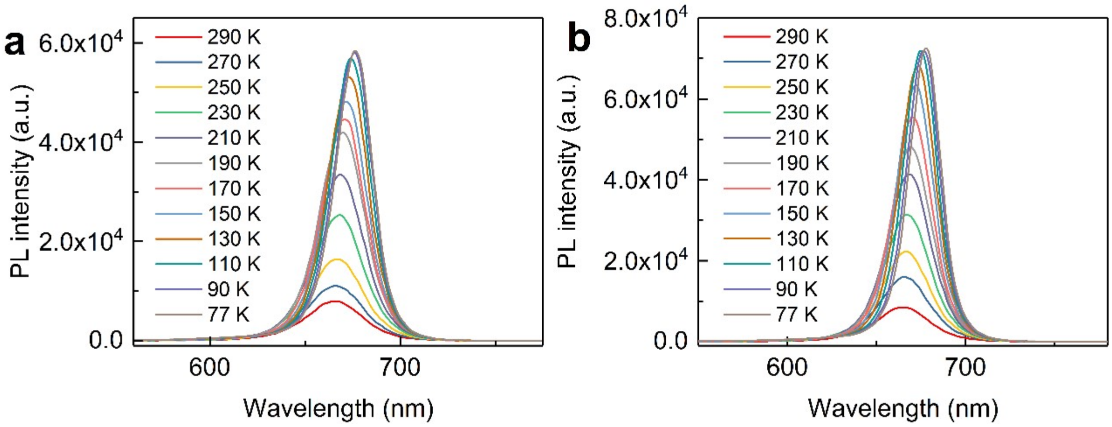

Figure S13. Temperature-dependent PL spectra of (a) pristine and (b) passivated $CsPbI_{3-x}Br_x$.

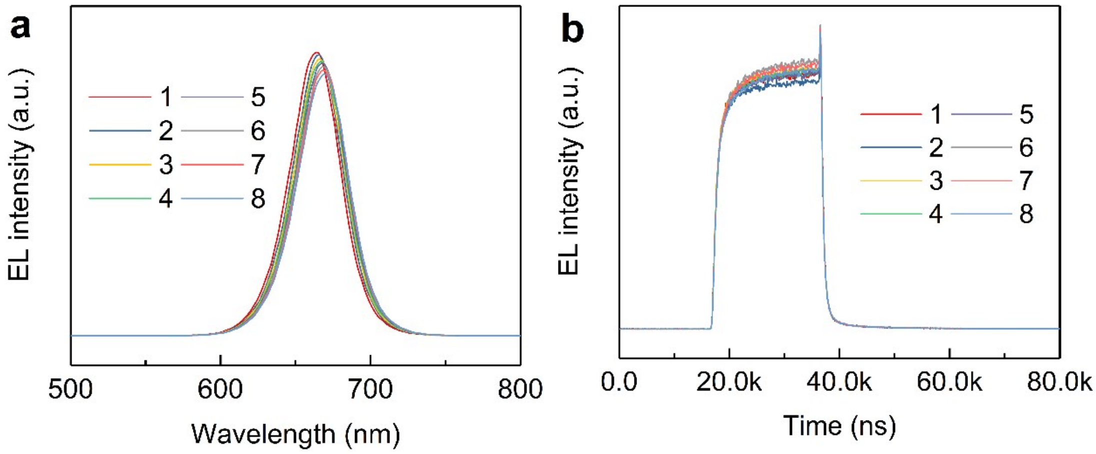

Figure S14. (a) Time-dependent EL spectrum and (b) time-dependent TRPL of passivated device. (testing every two minutes)

Table S1. Fitting parameters of the PL decay lifetime for the pristine $CsPbI_{3-x}Br_x$ and ZnI_2-passivated $CsPbI_{3-x}Br_x$ films with different molar ratio of Zn/Pb.

Perovskite	τ_1 [ns]	τ_2 [ns]	τ_3 [ns]	τ_{ave} [ns]
0.0 % (Pristine)	4.83	30.15	146.27	75.81
0.5%	5.19	33.34	168.70	96.82
1.0%	5.27	33.98	167.48	100.92
1.5%	4.10	26.48	142.02	94.51

Table S2. Device performances of red emission PeLEDs based on ZnI_2-passivated $CsPbI_{3-x}Br_x$ perovskite films.

Devices	V_{on} [V]	EL peak [nm]	L_{max} [cd m^{-2}]	EQE_{max} [%]	CE_{max} [cd A^{-1}]	T_{50} * [h]
Pristine	2.75	666	2020	6.94	1.46	2269.0
ZnI_2-passivated	2.70	666	4258	9.93	2.66	2667.0

* The initial luminance is 100 cd m^{-2}.

Table S3. Calculated formation energies (in eV) for defects in Zn doped $CsPbI_2Br$ at the three selected points A, B and C in **Figure S6**.

	A	**B**	**C**
Cs substitution	0.84	3.060814	5.279681
Pb substitution	4.30	2.09	-0.12

Table S4. The summarization of the performances of all-inorganic red emission PeLEDs with perovskite NCs or perovskite films emitters (the peak wavelength is from 630 nm to 700 nm).

Perovskite Material	Device Structure	Device Performance Parameters					Ref.
		EL (nm)	EQE (%)	L_{max} (cd m^{-2})	η_{CE} (cd A^{-1})	V_{on} (V)	
$CsPb(Br/I)_3$ NCs	ITO/ZnO-PEI /Perovskite NCs/CBP/TCTA/MoO_x/Au	648	6.30	2216	6.42	1.9	(1)
$NMA_2Cs_{n-1}Pb_nI_{3n+1}$	ITO/ ZnO/ PEIE/Perovskite/ TFB/MoO_x/Au	689	3.7	440	-	2.0	(2)
$PBA_2Cs_{n-1}Pb_nI_{3n+1}$	ITO/NiO/TFB/PVK/Perovskite/TPBi/Ca/Al	683	7.3	~100	-	~3.2	(3)
PEO/α-$CsPbI_3$	ITO/ZnO/PEI/Perovskite/ Poly-TPD/WO_3/Al	695	1.12	101	-	4.7	(4)
$CsPbI_3$ NCs (IDA-treated)	ITO/PEDOT:PSS/Poly-TPD/ Perovskite NCs/TPBi/LiF/Al	688	5.02	748	-	4.1	(5)
$CsPb(Br/I)_3$ NCs	ITO/PEDOT:PSS/Poly-TPD/ Perovskite NCs/TPBi/Liq/Al	645 653	14.1 21.3	794 500	11.6 10.6	2.7 2.8	(6)
$CsPb(Br/I)_3$ NCs	ITO/PEDOT:PSS/Poly-TPD/ Perovskite NCs/TPBi/Liq/Al	637	3.55	2671	2.97	3.6	(7)
$BA2Cs_{n-1}Pb_nI_{3n+1}$/ PEO	ITO/PEDOT:PSS/Poly-TPD/ Perovskite/BCP/LiF/Al	680	6.23	1392	1.71	~2.6	(8)
$NMA_2Cs_{n-1}Pb_nI_{3n+1}$	ITO/ ZnO/ PEIE/ Perovskite/TFB/MoO_x/Au	694	7.3	732	0.36	1.9	(9)
PEOXA/$CsPbBr_{0.6}I_{2.4}$	ITO/ZnMgO/Perovskite/ Poly-TPD/MoO_3/Ag	668	6.55	338	1.36	1.5	(10)
Ag-doped $CsPbI_3$ NCs	Ag/PEDOT:PSS/Perovskite NCs/TCTA/MoO_3/Au	690	11.2	1106	-	2.5	(11)
$PBA_2Cs_{n-1}Pb_nI_{3n+1}$	ITO/PEDOT:PSS/Poly-TPD/ PVK/Perovskite/TPBi/LiF/Al	664	13.3	968	-	2.6	(12)
$CsPb_{0.64}Zn_{0.36}I_3$ NCs	ITO/ZnO/ PEI/Perovskite NCs/TCTA/MoO_3/Au	668	15.1	2202	-	2.0	(13)
NEA/α-$CsPbI_3$	ITO/PEDOT:PSS/PVK/ Perovskite/TPBi/LiF/Al	682	8.65	210	-	2.8	(14)
$CsPb(Br_{0.43}I_{0.57})_3$	ITO/PTAA/PEDOT:PSS/ Perovskite/TPBi/LiF/Al	664	0.8	2765	0.84	2.5	(15)
4-F-PMAI/ $CsPbI_{2.8}Br_{0.2}$	ITO/Poly-TPD/Perovskite/ TPBi/LiF/Al	689	18.6	~60	-	~3.0	(16)

$PEA_2Cs_{n-1}Pb_nI_{3n+1}$ (Addition of ZnI_2)	ITO/PEDOT:PSS/Perovskite/ TPBi/LiF/Al	666	9.93	4258	2.66	2.8	This work

References:

[1] Zhang, X.; Sun, C.; Zhang, Y.; Wu, H.; Ji, C.; Chuai, Y.; Wang, P.; Wen, S.; Zhang, C.; Yu, W. W., Bright Perovskite Nanocrystal Films for Efficient Light-Emitting Devices. *J. Phys. Chem. Lett.* **2016***, 7,* 4602−4610.

[2] Zhang, S.; Yi, C.; Wang, N.; Sun, Y.; Zou, W.; Wei, Y.; Cao, Y.; Miao, Y.; Li, R.; Yin, Y.; Zhao, N.; Wang, J.; Huang, W., Efficient Red Perovskite Light-Emitting Diodes Based on Solution-Processed Multiple Quantum Wells. *Adv. Mater.* **2017***, 29,* 1606600.

[3] Si, J.; Liu, Y.; He, Z.; Du, H.; Du, K.; Chen, D.; Li, J.; Xu, M.; Tian, H.; He, H.; Di, D.; Lin, C.; Cheng, Y.; Wang, J.; Jin, Y., Efficient and High-Color-Purity Light-Emitting Diodes Based on In Situ Grown Films of $CsPbX_3$ (X = Br, I) Nanoplates with Controlled Thicknesses. *ACS Nano* **2017***, 11,* 11100−11107.

[4] Jeong, B.; Han, H.; Choi, Y. J.; Cho, S. H.; Kim, E. H.; Lee, S. W.; Kim, J. S.; Park, C.; Kim, D.; Park, C., All-Inorganic $CsPbI_3$ Perovskite Phase-Stabilized by Poly (ethylene oxide) for Red-Light-Emitting Diodes. *Adv. Funct. Mater.* **2018***, 28,* 1706401.

[5] Pan, J.; Shang, Y.; Yin, J.; De Bastiani, M.; Peng, W.; Dursun, I.; Sinatra, L.; El-Zohry, A. M.; Hedhili, M. N.; Emwas, A. H.; Mohammed, O. F.; Ning, Z.; Bakr, O. M., Bidentate Ligand-Passivated $CsPbI_3$ Perovskite Nanocrystals for Stable Near-Unity Photoluminescence Quantum Yield and Efficient Red Light-Emitting Diodes. *J. Am. Chem. Soc.* **2018***, 140,* 562−565.

[6] Chiba, T.; Hayashi, Y.; Ebe, H.; Hoshi, K.; Sato, J.; Sato, S.; Pu, Y.-J.; Ohisa, S.; Kido, J., Anion-exchange red perovskite quantum dots with ammonium iodine salts for highly efficient light-emitting devices. *Nat. Photonics* **2018***, 12,* 681−687.

[7] Yang, J. N.; Song, Y.; Yao, J. S.; Wang, K. H.; Wang, J. J.; Zhu, B. S.; Yao, M. M.; Rahman, S. U.; Lan, Y. F.; Fan, F. J.; Yao, H. B., Potassium Bromide Surface Passivation on $CsPbI_{3-x}Br_x$ Nanocrystals for Efficient and Stable Pure Red Perovskite

Light-Emitting Diodes. *J. Am. Chem. Soc.* **2020***, 142,* 2956−2967.

[8] Tian, Y.; Zhou, C.; Worku, M.; Wang, X.; Ling, Y.; Gao, H.; Zhou, Y.; Miao, Y.; Guan, J.; Ma, B., Highly Efficient Spectrally Stable Red Perovskite Light-Emitting Diodes. *Adv. Mater.* **2018***, 30,* 1707093.

[9] Chang, J.; Zhang, S.; Wang, N.; Sun, Y.; Wei, Y.; Li, R.; Yi, C.; Wang, J.; Huang, W., Enhanced Performance of Red Perovskite Light-Emitting Diodes through the Dimensional Tailoring of Perovskite Multiple Quantum Wells. *J. Phys. Chem. Lett.* **2018***, 9,* 881−886.

[10] Cai, W.; Chen, Z.; Li, Z.; Yan, L.; Zhang, D.; Liu, L.; Xu, Q. H.; Ma, Y.; Huang, F.; Yip, H. L.; Cao, Y., Polymer-Assisted In Situ Growth of All-Inorganic Perovskite Nanocrystal Film for Efficient and Stable Pure-Red Light-Emitting Devices. *ACS Appl. Mater. Interfaces* **2018***, 10,* 42564−42572.

[11] Lu, M.; Zhang, X.; Bai, X.; Wu, H.; Shen, X.; Zhang, Y.; Zhang, W.; Zheng, W.; Song, H.; Yu, W. W.; Rogach, A. L., Spontaneous Silver Doping and Surface Passivation of $CsPbI_3$ Perovskite Active Layer Enable Light-Emitting Devices with an External Quantum Efficiency of 11.2. *ACS Energy Lett.* **2018***, 3,* 1571−1577.

[12] He, Z.; Liu, Y.; Yang, Z.; Li, J.; Cui, J.; Chen, D.; Fang, Z.; He, H.; Ye, Z.; Zhu, H.; Wang, N.; Wang, J.; Jin, Y., High-Efficiency Red Light-Emitting Diodes Based on Multiple Quantum Wells of Phenylbutylammonium-Cesium Lead Iodide Perovskites. *ACS Photonics* **2019***, 6,* 587−594.

[13] Shen, X.; Zhang, Y.; Kershaw, S. V.; Li, T.; Wang, C.; Zhang, X.; Wang, W.; Li, D.; Wang, Y.; Lu, M.; Zhang, L.; Sun, C.; Zhao, D.; Qin, G.; Bai, X.; Yu, W. W.; Rogach, A. L., Zn-Alloyed $CsPbI_3$ Nanocrystals for Highly Efficient Perovskite Light-Emitting Devices. Nano Lett. **2019***, 19,* 1552−1559.

[14] Han, B.; Cai, B.; Shan, Q.; Song, J.; Li, J.; Zhang, F.; Chen, J.; Fang, T.; Ji, Q.; Xu, X.; Zeng, H., Stable, Efficient Red Perovskite Light-Emitting Diodes by (α, δ)-$CsPbI_3$ Phase Engineering. *Adv. Funct. Mater.* **2018***, 28,* 1804285.

[15] Guo, S.; Liu, Y. F.; Liu, Y. S.; Feng, J.; Sun, H. B., Improved performance of pure red perovskite light-emitting devices based on $CsPb(Br_{1-x}I_x)_3$ with variable content of iodine and bromine. *Opt Lett.* **2020***, 45,* 2724−2727.

[16] Cheng, G.; Liu, Y.; Chen, T.; Chen, W.; Fang, Z.; Zhang, J.; Ding, L.; Li, X.; Shi, T.; Xiao, Z., Efficient All-Inorganic Perovskite Light-Emitting Diodes with Improved Operation Stability. *ACS Appl. Mater. Interfaces* **2020**, *12,* 18084−18090.